

Numerical saddle point finding for diffusive superconductor actions

P. Virtanen¹

¹*Department of Physics and Nanoscience Center, University of Jyväskylä,
P.O. Box 35 (YFL), FI-40014 University of Jyväskylä, Finland*

We describe a numerical approach to modeling magnetoelectric effects generated by spin-orbit coupling in inhomogeneous diffusive 2D superconductors. It is based on direct minimization of the free energy of diffusion modes, including their coupling to the spin-orbit field strength, described by a recently discovered σ -model action. We explain how to retain exact conservation laws in the the discretized model, and detail the numerical procedure. We apply the approach to the spin-galvanic and the inverse spin-galvanic effects in finite-size 2D superconductors, and describe short-range oscillations of circulating currents and spin densities originating from the spin-orbit coupling.

I. INTRODUCTION

Breaking simultaneously the inversion and the time-reversal symmetries in a superconductor allows for several magnetoelectric effects. [1, 2] This includes spin-galvanic coupling between charge and spin degrees of freedom, [3–7] the φ_0 -effect and helical phases, [8–11] and the supercurrent diode effect [12–19]. One source for these effects arises from spin-orbit coupling (SOC) enabled by inversion symmetry breaking in the material. The theory for it in superconductors is most developed for homogeneous bulk superconductors, and ballistic systems without disorder or systems where Ginzburg–Landau type expansions are applicable. The other limit of disordered (“dirty”) inhomogeneous superconductors at low temperatures [20, 21] has also been extended to a description of different magnetoelectric effects originating from SOC [7, 22–26].

Recently in Refs. 24 and 27 we suggested that various SOC-generated magnetoelectric effects in dirty superconductors are captured by a σ -model [28–32] with one additional term in the action. However, despite the concise nature of such formulations, they might appear a somewhat cumbersome starting point compared to the quantum kinetic equations [20] traditionally used in superconductivity theory.

In this work we demonstrate that a formulation of the problem in terms of the action instead of the kinetic equations arising from it is immediately useful in numerical approaches, after a suitable discretization, which is the only manual step. The action formulation also enables us to conveniently find a discretization that preserves local gauge symmetries of the original model, and satisfies exact conservation laws. We apply the method to the equilibrium spin-galvanic effect and its inverse in 2D Rashba superconductors, and discuss resulting spatial spin density oscillations at sample boundaries.

In Sec. II, we recall the equilibrium version of the theory of Ref. 24. In Sec. III we formulate a symmetry-preserving discretization and the numerical solution strategy. In Sec. IV we apply the numerical method to spin-galvanic effects. Section V concludes the discussion.

II. MODEL

We consider a metallic system, whose normal state Hamiltonian contains a linear-in-momentum spin-orbit coupling (SOC) and an exchange field. It can be written as

$$H_0 = \frac{\hat{\mathbf{p}}^2}{2m} - \frac{1}{2m} \mathcal{A}_k^a \hat{p}_k \sigma^a - \frac{1}{2} \mathcal{A}_0^a \sigma^a + V_{\text{imp}}. \quad (1)$$

Here \hat{p}_k is the momentum in direction k for an electron with mass m , σ^a are the Pauli matrices in spin space ($k, a = x, y, z$), and V_{imp} is the random impurity potential. \mathcal{A}_k^a are the SU(2) potentials [33–39] describing the spin-orbit coupling, and \mathcal{A}_0^a describes the exchange field in direction a .

To describe superconductivity, this extends to the equivalent Bogoliubov–de Gennes Hamiltonian

$$\mathcal{H} = \tau_3 \left[\frac{\hbar^2 [\hat{\mathbf{k}} - \check{\mathbf{A}}(\mathbf{r})]^2}{2m} - \mu + V_{\text{imp}}(\mathbf{r}) - \check{A}_0(\mathbf{r}) - \hat{\Delta}(\mathbf{r}) \right], \quad (2)$$

where $\hat{\Delta}(\mathbf{r})$ is the superconducting pair potential. We are interested in the case where the impurity scattering V_{imp} is strong, and the system is in the diffusive transport regime, where mean free path ℓ is much longer than Fermi wavelength k_F^{-1} , but much smaller than other length scales.

An effective action describing the disorder-averaged physics of the above model was introduced in Ref. [24],

$$S[Q] = \frac{i\pi}{8} \text{Tr} \left[\frac{\sigma_{xx}}{2} (\hat{\nabla} Q)^2 + 4i\nu\Omega Q - \frac{\sigma'_{xy}}{2} iF_{ij} Q \hat{\nabla}_i Q \hat{\nabla}_j Q \right], \quad (3)$$

where ν is the density of states at Fermi level, $\sigma_{xx} = 2\nu D$ the longitudinal conductivity where D is the diffusion constant, and $\sigma'_{xy} = \frac{d\sigma_{xy}}{dB}|_{B=0} = 2\nu D\ell^2/(k_F\ell)$ the zero-field derivative of the Hall conductivity. We use units with $e = \hbar = 1$. The spin-orbit coupling enters via the covariant derivatives $\hat{\nabla}_i = \partial_{r_i} - i[\check{A}_i, \cdot]$ that include both $U(1)$ and $SU(2)$ vector potentials, and the corresponding field strength $F_{ij} = \partial_{r_i} \check{A}_j - \partial_{r_j} \check{A}_i - i[\check{A}_i, \check{A}_j]$. Moreover, $\Omega = \epsilon\tau_3 + \hat{\Delta} + \check{A}_0$, and superconductivity enters via the

anomalous self-energy $\hat{\Delta} = \tau_3(\tau_+\Delta + \tau_-\Delta^\dagger)$ where $\tau_\pm = \frac{1}{2}(\tau_1 \pm \tau_2)$ are combinations of the Pauli matrices $\tau_{1,2,3}$ in the Nambu space, and Δ is the superconducting order parameter.

The total action can also contain the mean-field interaction term $S_\Delta[\hat{\Delta}]$, which describes the interaction generating superconductivity. We could also include e.g. spin relaxation terms [29] such as $S_s[Q] = \frac{i\pi\nu}{8} \text{Tr}[\frac{1}{\tau_s}(\tau_3 \sigma Q)^2 + \frac{1}{\tau'_{so}}(\sigma Q)^2]$, describing spin relaxation by magnetic impurities and spin-orbit scattering.

We will consider here an equilibrium situation on the saddle point level. As the derivation of the action on this level is the same regardless of whether Keldysh or Matsubara formulation is used, in this case we can switch to a Matsubara formulation. [31] Then, the saddle-point values $Q = Q(\mathbf{r}, \omega_n)$ are functions of position, diagonal in Matsubara frequency [40] and constant in replica indices. They are 4×4 matrices in the Nambu \otimes spin space, with the property $Q(\mathbf{r}, \omega_n)^2 = 1$. Moreover, $\text{Tr } X = \int d^d r T \sum_{\omega_n} \text{tr } X(\mathbf{r}, \omega_n)$ contains summations over Matsubara frequencies and integration over material volume, in addition to matrix traces. The time derivative term is replaced by the imaginary time term $\epsilon = -i\omega_n$. Then $F = -iS$ is the free energy, and equilibrium configuration is found at its minimum.

The free energy is invariant with respect to “gauge transformations” $Q \mapsto UQU^{-1}$, $\check{\mathbf{A}} \mapsto U^{-1}\check{\mathbf{A}}U - iU^{-1}\hat{\nabla}U$ and $\epsilon\tau_3 + \hat{\Delta} \mapsto U^{-1}(\epsilon\tau_3 + \hat{\Delta})U$ where U is an invertible 4×4 matrix. This property is associated with conservation laws for charge and spin.

The charge J^c and spin J^s [38] currents are found by taking derivatives with respect to the potentials,

$$\mathcal{J}_\mu \equiv -\frac{2}{i\pi\nu} \frac{\delta S}{\delta \check{A}_\mu}, \quad (4)$$

$$J_i^c = -\frac{\pi\nu}{2} \text{Tr } \tau_3 \mathcal{J}_i, \quad (5)$$

$$J_{ij}^s = -\frac{\pi\nu}{2} \text{Tr } \sigma_j \mathcal{J}_i. \quad (6)$$

Similarly, the local spin and charge accumulations are given by

$$S_i = -\frac{\hbar}{2} \frac{\pi\nu}{2} \text{Tr } \sigma_i \tau_3 \mathcal{J}_0 = \frac{i\pi\nu}{4} \text{Tr } \sigma_i \tau_3 Q, \quad (7)$$

$$\delta\rho = -\frac{\pi\nu}{2} \text{Tr } \mathcal{J} = \frac{i\pi\nu}{2} \text{Tr } Q = 0. \quad (8)$$

In general $\delta\rho = 0$ in the equilibrium situation, as we are considering the metallic regime where the system is charge neutral.

Different types of boundaries of the system can be described with surface terms S_b in the action, e.g. corresponding to tunnel junctions [41–43]. Clean connections to large reservoirs may be modeled with a simpler rigid-boundary approximation, [44] where the value of $Q(\mathbf{r})$ in some region is taken as fixed. Moreover, restricting the space integral in Tr to a finite volume generates natural vacuum boundary conditions with $S_b = 0$.

III. METHOD

We now wish to find the values $Q_{ij}(\mathbf{r}, \omega_n)$ that solve the saddle-point equation:

$$\frac{\delta S}{\delta Q_{ij}(\mathbf{r}, \omega_n)} = 0. \quad (9)$$

As we consider interactions only on the mean-field level (i.e., weak-coupling superconductivity), the saddle-point equations do not mix different Matsubara frequency components together, and each may be solved separately.

In addition, we need to compute the values of the currents and densities (4,7).

A. Gauge-invariant discretization

We will in general find the minimum of Eq. (3) numerically (implementation is available [45]), which requires discretization of the continuum action. Naive discretization does not preserve the covariant conservation law of the spin current. Moreover, given the presence of the magnetoelectric coupling (Hall term), also charge conservation can be broken. Although the magnitude of the discretization artifacts in the conservation laws should in general decrease as the lattice spacing is reduced, this can occur slowly. To preserve conservation laws exactly, it is advantageous to formulate the problem in such a way that a discrete version of the gauge invariance is retained. Such approach is commonly used in lattice gauge theories [46], and it is useful also for the case here where the “gauge field” is fixed.

We discretize the action as follows. We subdivide the space to rectangular cells, centered on a lattice $\mathbf{r}_j = (hj_x, hj_y, hj_z)$ with $j_{x,y,z} \in \mathbb{Z}$ and h is the lattice spacing. We choose $Q_j = Q(\mathbf{r}_j)$ to be the values of Q at the lattice sites. We define the Wilson link matrices connecting neighboring sites $U_{ij} = U_{ji}^{-1} = U(\mathbf{r}_i, \mathbf{r}_j) = \text{Pexp}[i \int_{L(\mathbf{r}_i, \mathbf{r}_j)} d\mathbf{r}' \cdot \check{\mathbf{A}}(\mathbf{r}')]]$ where $L(\mathbf{r}_i, \mathbf{r}_j)$ is the straight line from \mathbf{r}_j to \mathbf{r}_i and Pexp is the path-ordered integral. They describe the parallel transport from one lattice site to another, and the gauge fields only appear via them. In our problem, the gauge field $\check{\mathbf{A}}$ is fixed, so the link matrices can be computed ahead of time.

We require that the discretized S is invariant under discrete local gauge transformations

$$\begin{aligned} Q_j &\mapsto u(j)Q_ju(j)^{-1}, & U_{ij} &\mapsto u(i)U_{ij}u(j)^{-1}, \\ \Omega_i &\mapsto u(i)\Omega_iu(i)^{-1}, \end{aligned} \quad (10)$$

for any set of transformation matrices $u(i)$ on each site. The term with the field-strength tensor F_{ij} in Eq. (3) can be expressed in terms of the link matrices U only, which guarantees it inherits the invariance from their transformation. Finally, we also require the result in the continuum limit reduces to Eq. (3).

From the definition of the current as a derivative with respect to the gauge potentials (4), one finds the discrete

current incoming from cell j measured at site i along the link (i, j) :

$$J_{ij}^a = \frac{\partial}{\partial \xi} S[U_{ij} \mapsto e^{\xi T^a} U_{ij}, U_{ji} \mapsto U_{ji} e^{-\xi T^a}]|_{\xi=0} \quad (11)$$

where T^a is an appropriate matrix generator of the current, $T^0 = \tau_3$ for the charge current and $T^{x,y,z} = \sigma_{x,y,z}$ for the spin current, and the transformation is made only in the link (i, j) .

The local gauge invariance (10) then implies that the model has an exact discrete continuity equation

$$R_i^a \equiv \sum_{j \in \text{neigh}(i)} J_{ij}^a \quad (12)$$

$$= \frac{\partial}{\partial \xi} S[Q_i \mapsto e^{-\xi T^a} Q_i e^{\xi T^a}, \Omega_i \mapsto e^{-\xi T^a} \Omega_i e^{\xi T^a}], \quad (13)$$

which defines the current sink term R_i^a . The ξ -dependent rotation of Q and $\hat{\Delta}$ can be eliminated with a change of variables, which moves it to S_s and S_Δ , and it remains in the \hat{A}_0 part of Ω . In particular, all parts are invariant under the rotations generated by T^0 , and hence charge current is conserved exactly. Generally, S_s is not SU(2) rotation invariant, and if $S_s \neq 0$, it will break the spin current conservation. Similar statement applies to \hat{A}_0 if it contains a spin-dependent part, i.e. an exchange field. S_Δ may also break spin current conservation if it describes spin-triplet superconductivity. Note that these conclusions required a change of variables, so that in saddle point equations they hold only when both Q and $\hat{\Delta}$ have their saddle-point values defined by $\frac{\delta}{\delta \hat{\Delta}}(S + S_\Delta + S_s) = \frac{\delta}{\delta Q}(S + S_\Delta + S_s) = 0$.

The spin current in this model is only covariantly conserved. [33, 34, 36, 38] This is here visible in the fact that the definition of the lattice spin current is not symmetric, so that $J_{ij} \neq -J_{ji}$. From Eq. (11) one can observe that the asymmetry is present only when T^a does not commute with U_{ij} . This is an issue only for the spin current, as the charge current generator $T^0 = \tau_3$ always commutes with U_{ij} . What this means is that since the parallel transport of spin between the sites i and j can imply spin rotation described by the gauge field, the currents measured at separated points are generally not equal.

We can then start constructing a discretization satisfying Eq. (10). We discretize the directional gradient $\mathbf{e}_{ij} \cdot \hat{\nabla} Q$ on a link between cells i and j as

$$D_{ij} := \frac{1}{h} (Q_i U_{ij} - U_{ij} Q_j). \quad (14)$$

This choice is useful, because in addition to the simple transformation law $D_{ij} \mapsto u(i) D_{ij} u(j)^{-1}$, it retains an exact “anticommutation” relation $Q_i D_{ij} = -D_{ij} Q_j$, analogous to the property $Q \hat{\nabla} Q = -(\hat{\nabla} Q)Q$ of the continuum derivative that arises due to the normalization $Q^2 = 1$. This ensures that the various equivalent continuum forms that can be constructed by re-ordering Q and $\hat{\nabla} Q$ have their corresponding equivalent

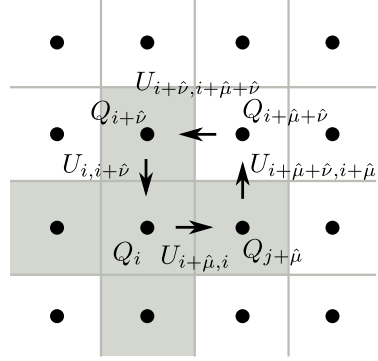


FIG. 1. Lattice discretization. Neighbors of site i are shaded, and the arrows indicate the plaquette loop P_{lkj_i} for the coordinate directions $\hat{\mu}$, $\hat{\nu}$.

forms in the discretized case. For $h \rightarrow 0$, one can verify that the above produces the correct continuum limit: $D_{ij} \rightarrow \frac{Q_i - Q_j}{h} - [i \mathbf{e}_{ij} \cdot \check{\mathbf{A}}(\frac{\mathbf{r}_i + \mathbf{r}_j}{2}), Q_j] \rightarrow \mathbf{e}_{ij} \cdot \hat{\nabla} Q$.

We then discretize

$$\text{Tr}(\hat{\nabla} Q)^2 \mapsto -\frac{2d}{|\text{neigh}|} h^d \sum_{\text{neigh}(i,j)} \text{Tr} D_{ij} D_{ji} \quad (15)$$

where d is the space dimension and $|\text{neigh}| = 2^d$ the number of neighbors of the cell on the lattice. From the transformation properties of D_{ij} , the above is invariant under Eq. (10).

The discretization of the field-strength $F_{\mu\nu}$ term can be made following similar ideas as in lattice QCD, where the gluon action is expressed in terms of the link matrices U via a plaquette loop [46]. Consider the plaquette (see Fig. 1), with corner site i and axes $\mu \neq \nu$, and denote $j = i + \hat{\mu}$, $k = i + \hat{\mu} + \hat{\nu}$, $l = i + \hat{\nu}$. Expand around $\mathbf{r}_0 = \frac{\mathbf{r}_i + \mathbf{r}_j + \mathbf{r}_k + \mathbf{r}_l}{4}$:

$$P_{lkj_i} := U_{il} U_{lk} U_{kj} U_{ji} = 1 + i h^2 F_{\mu\nu}(\mathbf{r}_0) + \mathcal{O}(h^3), \quad (16)$$

which then provides an expression for F in terms of the link matrices U . The above expansion follows from the continuum limit expansion of the link matrices

$$U_{ji} = \sum_{n=0}^{\infty} i^n |\mathbf{r}_i - \mathbf{r}_j|^n \int_{-1/2}^{1/2} ds_1 \int_{-1/2}^{s_1} ds_2 \dots \int_{-1/2}^{s_{n-1}} ds_n \times \mathcal{A}(s_1) \dots \mathcal{A}(s_n), \quad (17)$$

where $\mathcal{A}(s) = \mathbf{e}_{ij} \cdot \check{\mathbf{A}}[(\frac{1}{2} - s)\mathbf{r}_i + (\frac{1}{2} + s)\mathbf{r}_j]$.

We can then express

$$\text{Tr} F_{\mu\nu} Q \hat{\nabla}_\mu Q \hat{\nabla}_\nu Q \mapsto \frac{i}{h^4} \text{Tr}(1 - P_{lkj_i}) U_{ij} D_{ji} Q_i D_{il} U_{li}. \quad (18)$$

This expression now both retains the discrete gauge invariance, and in the continuum limit reduces to the correct term. Summation over the μ , ν indices must also be done. To avoid directionality bias, we express

it as an average over the corners of the plaquettes as follows. This gives a discretization of the Hall term $S_H = \text{Tr } F_{ij} Q \hat{\nabla}_i Q \hat{\nabla}_j Q$:

$$S_H \mapsto \frac{h^d d}{4i h^4} \sum_{\text{plaqc}(ijkl; i)} \text{Tr}(U_{lk} U_{kj} - U_{li} U_{ij}) D_{ji} Q_i D_{il}, \quad (19)$$

where $\text{plaqc}(ijkl; i)$ implies summation over all plaquettes surrounding all corner sites i .

The discretization of the remaining local terms is straightforward, and can be done as $\text{Tr } \Omega Q \mapsto \sum_i h^d \text{Tr}(\Omega_i Q_i)$.

B. Numerical implementation

In the typical numerical approach, one would now try to manually evaluate the variation $\delta S / \delta Q$ to find the saddle-point (Usadel) equations, and then attempt to solve them with a Newton method or some other approach. This is somewhat unwieldy here.

However, we can also approach this as a general nonlinear minimization problem of the free energy, and in particular, make use of algorithmic differentiation methods. The advantage here is that they require as an input only a computer routine evaluating the discretized free energy, given variables $\{Q_j\}$ as input. The first (gradient) and second (Hessian) derivatives of the discretized S with respect to the input variables can then be automatically deduced, allowing the use of efficient gradient-based optimization methods.

In practice, all manual symbolic manipulation necessary is then already completed in the previous section. Hence, we have an essentially *action-based* numerical method, where it would be very simple to e.g. include additional terms in Eq. (3) if needed. The discrete gauge invariance also implies the approach is not sensitive to the gauge choices, and satisfies conservation laws exactly.

We use the CppAD library [47] for computing the gradient and Hessian of S with respect to the input variables. Moreover, it is also used to evaluate the action derivatives giving the currents (4).

The Matsubara sums are evaluated using a Gaussian sum quadrature [48],

$$\sum_{n=-\infty}^{\infty} f(\omega_n) \simeq \sum_{j=1}^N \tilde{a}_j f(\tilde{\omega}_j(T)), \quad (20)$$

where \tilde{a}_j and $\tilde{\omega}_j(T) = 2\pi T(\tilde{n}_j + \frac{1}{2})$ are such that the equality is exact for any functions $f(\omega_n)$ that are polynomials in $(1 + |\omega_n|)^{-2}$ of order less than $N/2$. Here, N is chosen such that the largest $\tilde{\omega}_j$ is much larger than the typical energy scale of $Q(\omega)$. The quadrature is generally more rapidly convergent than naive summation, and moreover ensures that also large values of ω are sampled without needing very large N .

The saddle-point equation $\delta S / \delta Q = 0$ is solved with a preconditioned Newton–Krylov method. [49] Parametrizing $\{Q_i\}$ in terms of real variables $\mathbf{x} = \{x_i\}$, this corresponds to iteration $\mathbf{x}^{(n+1)} = \mathbf{x}^{(n)} + \delta \mathbf{x}^{(n)}$, where a Krylov method solves the problems

$$M \frac{\partial^2 S[\mathbf{x}^{(n)}]}{\partial \mathbf{x} \partial \mathbf{x}} \delta \mathbf{x}^{(n)} = -M \frac{\partial S[\mathbf{x}^{(n)}]}{\partial \mathbf{x}}, \quad (21)$$

where $\partial S / \partial \mathbf{x} \partial \mathbf{x}$ is the Hessian and $\partial S / \partial \mathbf{x}$ the gradient of S with respect to the real input variables. We use a number of standard approaches to accelerate the solution. The preconditioner M is taken to be the (incomplete) sparse LU inverse [50] of the Hessian. Updating the Hessian is an expensive step in the calculation, and in general we keep M “frozen” for several iterations and recompute it only if the Krylov convergence starts to suffer. Computation of the Hessian is avoided in the Krylov steps themselves, as they only require the matrix–vector products $(\partial S / \partial \mathbf{x} \partial \mathbf{x}) \mathbf{y} \simeq \frac{1}{\alpha} (\frac{\partial S}{\partial \mathbf{x}}[\mathbf{x}^{(n)}] + \alpha \mathbf{y}) - \frac{\partial S}{\partial \mathbf{x}}[\mathbf{x}^{(n)}]$, which can be computed as numerical derivatives of the gradient with $\alpha \rightarrow 0$.

The conditions $Q_i^2 = 1$ are here eliminated by a Riccati parametrization of the matrix Q_i , in terms of unconstrained complex 2×2 matrices γ and $\tilde{\gamma}$:

$$Q_i = \begin{pmatrix} 1 + \gamma_i \tilde{\gamma}_i & 0 \\ 0 & 1 + \tilde{\gamma}_i \gamma_i \end{pmatrix}^{-1} \begin{pmatrix} 1 - \gamma_i \tilde{\gamma}_i & 2\gamma_i \\ 2\tilde{\gamma}_i & -1 + \tilde{\gamma}_i \gamma_i \end{pmatrix}. \quad (22)$$

The real variables \mathbf{x} are then the real and imaginary parts of the matrix elements of γ_i and $\tilde{\gamma}_i$ in each cell in the discretization.

C. Superconducting interaction

We consider here only BCS singlet weak-coupling superconductivity. Its interaction term can be taken as

$$S_\Delta = \frac{1}{2\lambda} \int d^d r \text{tr}[\hat{\Delta}^\dagger \hat{\Delta}], \quad (23)$$

where λ is an interaction constant, and $\hat{\Delta}$ is assumed to contain only the singlet, $\hat{\Delta} \propto \sigma_0$.

To deal with the BCS cutoff, we use the usual cutoff elimination by adding and subtracting

$$\begin{aligned} & -\frac{\pi\nu}{8} \text{Tr}[4(\omega \hat{\tau}_3 - i\hat{\Delta})Q] + S_\Delta = \\ & -\frac{\pi\nu}{2} \text{Tr}[(\omega_n \hat{\tau}_3 - i\hat{\Delta})(Q - \hat{\tau}_3) - \frac{\hat{\Delta}^\dagger \hat{\Delta}}{|\omega_n|}] + S'_\Delta, \end{aligned} \quad (24)$$

where the part in $\text{Tr}[\dots]$ contains a convergent Matsubara sum at the saddle point Q_* as the slowly decaying part in Q_* at $|\omega_n| \rightarrow \infty$ is canceled, and

$$S'_\Delta = \frac{\nu}{2} \left(\frac{1}{\nu\lambda} - \pi T \sum_{|\omega_n| < \omega_c} \frac{1}{|\omega_n|} \right) \int d^d r \text{tr}[\hat{\Delta}^\dagger \hat{\Delta}] \quad (25)$$

$$\simeq \frac{\nu}{2} \log \left(\frac{T}{T_{c0}} \right) \int d^d r \text{tr}[\hat{\Delta}^\dagger \hat{\Delta}], \quad (26)$$

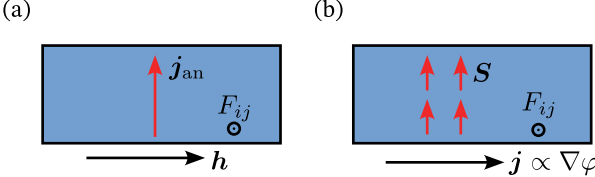


FIG. 2. (a) Spin-galvanic effect: anomalous charge current j_{an} generated by the Rashba SOC field strength F_{ij} and an exchange field \mathbf{h} . (b) Inverse spin-galvanic effect: spin density \mathbf{S} generated by F_{ij} and charge supercurrent \mathbf{j} . Both effects are perturbed by finite sample boundaries.

where $T_{c0} = (2e^\gamma \omega_c / \pi) e^{-1/(\lambda\nu)} = (e^\gamma / \pi) \Delta_0$ is the BCS critical temperature.

IV. MAGNETOELECTRIC RESPONSE

The spin-orbit coupling results to several magnetoelectric effects in superconductors. One of them is the spin-galvanic or inverse Edelstein effect, generation of anomalous equilibrium supercurrents due to external Zeeman fields, and its inverse effect. [3–5, 10] These are schematically illustrated in Fig. 2.

A. Spin-galvanic effect

Consider a finite-size 2D superconducting layer of size $L \times W$, with Rashba spin-orbit coupling $\check{A}_x = \alpha\sigma_y$, $\check{A}_y = -\alpha\sigma_x$, $F_{ij} = 2\alpha^2\sigma_z\epsilon_{ijz}$, and an internal exchange field $\mathbf{h} = h\hat{x}$. In this configuration, the magnetoelectric coupling generates equilibrium supercurrents, whose flow is restricted by the sample boundaries. These effects were previously theoretically studied in Ref. [51], based on linearized equations that are valid for weak fields $h \rightarrow 0$, and with an analysis of the resulting magnetoelectric currents on length scales long compared to the coherence length ξ_0 . The latter approximation results to an oversimplification of the currents when either W or L is of the order of ξ_0 , discussed in more detail below.

We can now solve the self-consistent problem for the discretized problem by minimizing the free energy in Q and Δ . We ignore electromagnetic self-field effects, so the result is valid in the limit of negligible magnetic screening, i.e., long Pearl length [52] $\Lambda = m/(e^2\mu_0 n_s) \gg L, W$.

To characterize the strength of the Rashba spin-orbit interaction and the magnetoelectric conversion, it is useful to introduce the following rates:

$$\Gamma_r = 4D\alpha^2, \quad \Gamma_{st} = \Gamma_r \frac{\ell^2\alpha}{k_F\ell\xi_0} = \frac{\Gamma_r^{3/2}\Delta_0^{1/2}}{2E_F}, \quad (27)$$

where $\xi_0 = \sqrt{D/\Delta_0}$ is the zero-temperature coherence length. Here, Γ_r is the prefactor of the Dyakonov-Perel spin-orbit relaxation term [29] $S = \dots +$

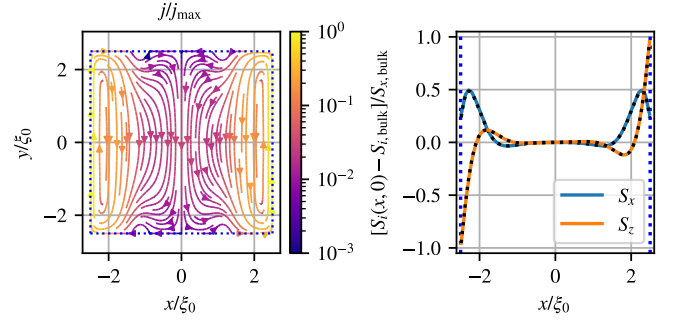


FIG. 3. Left: Current flow for $\Gamma_r = 10\Delta_0$, $\Gamma_{st} = 0.4\Delta_0$, $T = 0.2\Delta_0$, $h = 0.1\Delta_0$, $L = 5\xi_0$, $W = 5\xi_0$, with grid size 60×60 . Line color indicates current amplitude $|\mathbf{j}|$. Right: Corresponding spin density oscillation at $y = 0$. Dotted black line is the $h \rightarrow 0$, $W \gg L$ limit analytical solution [51].

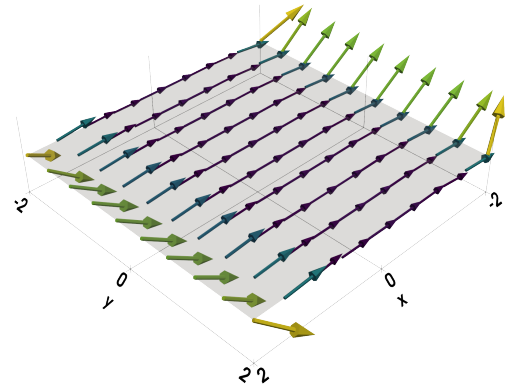


FIG. 4. Spin texture corresponding to Fig. 3.

$\frac{i\pi\nu}{8} \text{Tr}[\frac{\Gamma_r}{2} \sum_{i=x,y} Q\sigma_i Q\sigma_i]$ that appears from the gradient term of the action. Moreover, $\Gamma_{st} = \frac{D\ell^2}{k_F\ell} 4\alpha^3\xi_0^{-1}$ indicates the strength of the singlet-triplet conversion cross-terms $\frac{d\sigma_{xy}}{dB} F_{ij}[-i\alpha\sigma, Q]\nabla_j Q \propto \Gamma_{st}$.

The calculated charge current and spin density S_x for a square sample $L = W = 10\xi_0$ are illustrated in Fig. 3. The spin density follows the small- h analytical result of Ref. 51 essentially exactly, except in the corners where

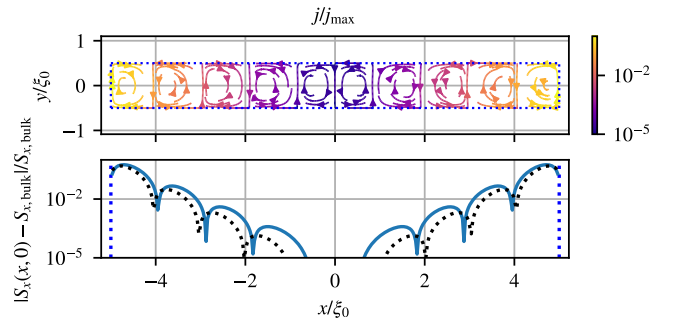


FIG. 5. Same as Fig. 3, but for $L = 10\xi_0$, $W = \xi_0$, with grid size 220×22 .

the spin texture tilts in y -direction, as seen in Fig. 4. The current is qualitatively similar to what is discussed in Ref. 51, however note the appearance of four “vortices” close to $x = 0$. This structure becomes more apparent for $L \gg W \sim \xi_0$, as shown in Fig. 5.

The result can be understood as follows. The spin-dependent gauge field A together with a sample boundary generates a perturbation in the triplet component \mathbf{Q}_t of $Q = Q_s + \mathbf{Q}_t \cdot \boldsymbol{\sigma}$, and also in the spin density. The perturbation has an oscillatory decay $\delta \mathbf{Q}_t \propto e^{-k_n x}$ from the boundary toward the bulk value, with the complex decay wave vectors [51]

$$ik_n^\pm = \sqrt{\kappa_n^2 - 2\alpha^2 \pm 2i\sqrt{7\alpha^2 + 4\kappa_n^2}}, \quad (28)$$

where $\kappa_n^2 = 2\sqrt{\omega_n^2 + \Delta^2}/D$. The F_{ij} SOC term couples these (spin) oscillations to the singlet (charge) sector. This is simplest to consider for weak superconductivity, $f, f^\dagger \rightarrow 0$:

$$Q \simeq \begin{pmatrix} 1 - \frac{1}{2}ff^\dagger & f \\ f^\dagger & -1 + \frac{1}{2}f^\dagger f \end{pmatrix}. \quad (29)$$

Writing $f = f_s + \mathbf{f}_t \cdot \boldsymbol{\sigma}$, $f^\dagger = f_s^\dagger + \mathbf{f}_t^\dagger \cdot \boldsymbol{\sigma}$ and assuming Rashba interaction, the singlet-triplet coupling term in the action becomes

$$S_{ST} = \frac{\pi\sigma'_{xy}}{4}\alpha^2 \text{Tr}[\partial_x f_t \partial_y f_s^\dagger - \partial_x f_t^\dagger \partial_y f_s - 2\alpha(\mathbf{f}_t \times \nabla f_s^\dagger) \cdot \hat{z} + 2\alpha(\mathbf{f}_t^\dagger \times \nabla f_s) \cdot \hat{z}]. \quad (30)$$

In Ginzburg–Landau expansion, $f_{s/t}(\mathbf{r}) = \Delta(\mathbf{r})\tilde{f}_{s/t}$, $f_{s/t}^\dagger = \Delta(\mathbf{r})^*\tilde{f}_{s/t}$, this produces a Lifshitz invariant [1]

$$S_{ST} = i(\boldsymbol{\eta} \times \hat{z}) \cdot (\Delta^* \nabla \Delta - \Delta \nabla \Delta^*), \quad (31)$$

where $\boldsymbol{\eta} \propto \alpha^3 \sum_{\omega_n} \tilde{f}_t \tilde{f}_s$. Then also $\boldsymbol{\eta} \approx \eta_y(x)\hat{y}$ oscillates as a function of distance from the surface, producing an effective magnetic field $\mathbf{B}_{\text{eff}}(x) = \hat{z}\partial_x \eta_y(x)$. This then results to the circulating currents visible in Fig. 5. Increasing the strip width results to averaging over these short-range oscillations, and gradually transforms the solution towards uniform current flow as seen in Fig. 3.

B. Inverse spin-galvanic effect

The converse to the above is the inverse spin-galvanic effect (ISGE) or Edelstein effect, where the singlet-triplet coupling generates a spin density from a charge current.

To find ISGE in a uniform infinite 2D strip of width W , we can assume a nonzero orbital field A_x driving current along the strip in x -direction. Then, $\hat{\nabla}_x Q = \partial_x Q - i[A_x \tau_3 + \alpha \sigma_y, Q]$, we can assume Δ is real, and find the solution $Q = Q(y)$ of the saddle-point equations. The Rashba coupling is as in the previous section, and we

take $h = 0$. The saddle point equations can be written as [24]

$$D\hat{\nabla}_i(Q\hat{\nabla}_i Q) - [\tilde{\Omega}, Q] = -\tilde{\eta}\mathcal{T}, \quad (32)$$

$$\mathcal{T} = \hat{\nabla}_i J_i^H, \quad \tilde{\Omega} = \omega_n \tau_3 + \Delta \tau_1, \quad (33)$$

$$J_i^H = \{F_{ij} + QF_{ij}Q, \hat{\nabla}_j Q\} - i\hat{\nabla}_j(Q[\hat{\nabla}_i Q, \hat{\nabla}_j Q]), \quad (34)$$

where $\tilde{\eta} = \frac{D\ell^2}{4k_F\ell} = \frac{D\tau}{4m} = \frac{\xi_0 \Gamma_{st}}{16\alpha^3}$. Analytical results can be found by working in the leading order in $\tilde{\eta}$ and A_x : assume $Q = Q_0 + \delta Q + \mathcal{O}(\tilde{\eta}^2, A_x^2)$, where $Q_0 = \tilde{\Omega}/\sqrt{\omega_n^2 + \Delta^2}$ is the equilibrium bulk solution, $\{Q_0, \delta Q\} = 0$, and $\delta Q \propto A_x \tilde{\eta}$. We have then $\hat{\nabla}_x Q_0 = -iA_x[\tau_3, Q_0] = 2A_x f_0 \tau_2$ and $\hat{\nabla}_y Q_0 = 0$, and $[F_{ij}, Q_0] = 0$. Also, δQ does not appear in \mathcal{T} in the leading order, so that

$$\mathcal{T} \simeq 2\{\hat{\nabla}_y F_{yx}, \hat{\nabla}_x Q_0\} = -32\alpha^3 A_x f_0 \sigma_y \tau_2, \quad (35)$$

where $f_0 = \Delta/\sqrt{\omega_n^2 + \Delta^2}$.

For $W \rightarrow \infty$, we can assume $\partial_y \delta Q = 0$, and $\delta Q \propto \sigma_y$. The spin relaxation term in Eq. (32) then obtains the form $D\hat{\nabla}_i(Q\hat{\nabla}_i Q) \simeq -\Gamma_r Q_0 \delta Q$. The equation is solved by $\delta Q = [\Gamma_r Q_0 + 2\tilde{\Omega}]^{-1} \tilde{\eta} \mathcal{T}$, i.e.,

$$\delta Q_{\text{bulk}} = \Gamma_{st} \xi_0 A_x \frac{i[\Delta \omega_n \tau_1 - \Delta^2 \tau_3] \sigma_y}{(\frac{1}{2}\Gamma_r + \sqrt{\omega_n^2 + \Delta^2})(\omega_n^2 + \Delta^2)}. \quad (36)$$

The induced bulk spin density is $\mathbf{S} = S_y \hat{y}$, where

$$S_y = \Gamma_{st} \xi_0 A_x \pi \nu T \sum_{\omega_n} \frac{\Delta^2}{(\frac{1}{2}\Gamma_r + \sqrt{\omega_n^2 + \Delta^2})(\omega_n^2 + \Delta^2)}. \quad (37)$$

As shown in [3], \mathbf{S} is perpendicular both to the Rashba direction $F_{ij} \propto \sigma_z$ and the current flow. This bulk value agrees with previous results [5, 7, 23].

The vacuum boundary conditions at $y = \pm W/2$ read:

$$J_{y,\text{tot}} = DQ(\partial_y Q - i[-\alpha \sigma_x, Q]) + \tilde{\eta} J_y^H = 0. \quad (38)$$

The bulk solution (36) does not satisfy it, resulting into a perturbation that decays towards the bulk similarly as seen in the previous section. From the spin structure of the equations, one can observe that the solution for δQ in leading order in $\tilde{\eta}$, A_x , should generally have the form $\delta Q = \delta Q_{\text{bulk}} + \tilde{Q}$, $\tilde{Q} = \tilde{Q}_y \sigma_y + \tilde{Q}_z \sigma_z$. Consequently, spin accumulation $S_z \neq 0$ can appear close to the strip edges, whereas $S_x = 0$.

We can proceed to solve the spin accumulation analytically. Working again the leading order in $\tilde{\eta}, A_x$, the boundary condition and Eq. (32) read

$$D(\partial_y + 2i\alpha \sigma_x)\tilde{Q} = 16\tilde{\eta} A_x \alpha^2 f_0 Q_0 \sigma_z \tau_2 - 2iD\alpha \sigma_x \delta Q_{\text{bulk}}, \quad (39)$$

$$D(\partial_y + 2i\alpha \sigma_x)^2 \tilde{Q} - \Gamma_r \frac{\tilde{Q} - \sigma_y \tilde{Q} \sigma_y}{2} - 2\sqrt{\omega_n^2 + \Delta^2} \tilde{Q} = 0. \quad (40)$$

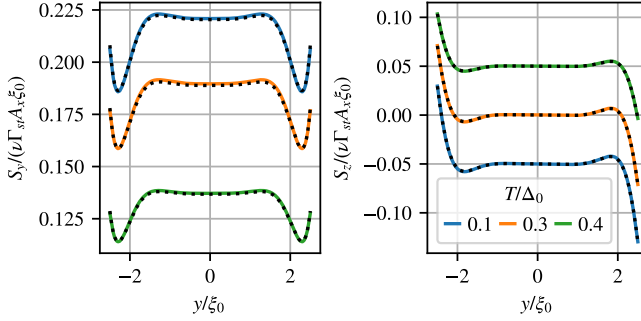


FIG. 6. Inverse spin-galvanic effect. Spin density at different temperatures is shown, for $A_x \xi_0 = 0.005$, $W = 5\xi_0$, $L = 4\xi_0$, $\Gamma_r = 10\Delta_0$, and $\Gamma_{st} = 0.4\Delta_0$, with grid size 90×90 . Left: S_y . Right: S_z (curves offset vertically by ± 0.05 for clarity). Solid lines indicate numerical results, black dotted lines solutions to Eq. (39).

The second equation has the general solution $\tilde{Q} = \sum_{ab=\pm} \tilde{Q}_{zab} [\sigma_z + B_n^b \sigma_y] e^{iak_n^b y}$, $B_n^b = -4\alpha i k_n^b / [(ik_n^b)^2 - 4\alpha^2 - \kappa_n^2]$, where k_n^\pm are given by Eq. (28). The coefficients \tilde{Q}_{zab} are determined by Eq. (39) at $y = \pm W/2$, and can be solved.

The resulting spin density and corresponding numerical results are shown in Fig. 6, for a finite-size case where $L, W > \xi_0$. At the left and right ends, we assume Q is fixed to the values $Q_0|_{\Delta \rightarrow \Delta e^{\pm i A_x L/2}}$ which in the self-consistent calculation generates a nearly uniform phase gradient along x . The numerical and analytical results for the spin density generated by the inverse galvanic effect agree for the small phase gradient A_x chosen.

Spin accumulation $S_z \neq 0$ at the boundaries in general could be expected to be generated by the spin-Hall effect [53]. However, in the leading order in $\tilde{\eta}$, the total matrix current in the bulk is $J_{y,\text{tot}} \propto \tau_2 \sigma_z$, and from Eq. (6) one finds $J_{ij}^s = 0$, i.e., no bulk spin current. The behavior here is then somewhat different from a spin-Hall effect, where bulk spin current is balanced by boundary spin accumulation and relaxation. In addition, in the system here $S_z \neq 0$ only in the superconducting state. In dirty 2D Rashba metals with a parabolic spectrum in the normal state the DC spin-Hall effect vanishes, and $S_z = 0$ at strip boundaries. [54, 55] This also follows from the present theory in the normal state: under similar approximation as above using the normal-state nonequilibrium form of the equations, [23, 24] one finds $J_{y,\text{tot}} = 0$ which also implies the vanishing spin-Hall effect [56].

V. SUMMARY AND CONCLUSIONS

We presented an approach where numerical saddle-point solutions to the spin-orbit coupled diffusion theory

in 2D superconductors are obtained relatively directly from the original action formulation. The formulation is constructed in such a way that it satisfies exact discrete versions of the conservation laws originating from symmetries in the original theory. We applied it to studying the spin-galvanic effects in finite-size Rashba superconductors, where the SOC and exchange field or charge currents interact with the sample boundaries, generating oscillations in the spin density. We considered these problems also analytically, and find that the numerical and analytical results fully agree in the validity range of the latter. For the inverse spin-galvanic effect, we find that equilibrium supercurrent does generate boundary spin accumulations qualitatively similar to the spin-Hall effect, even though quasiparticle current in the same system in the normal state does not.

The approach is not limited to the specific model and effects considered above. It can be applied also to studying the superconducting diode effect in the dirty limit [26], or spin-orbit effects in multiterminal structures. A nonequilibrium version can be used to model the quasiparticle spin-Hall effect [53], and its interaction with other nonequilibrium effects in spin-split superconductors. [57] Moreover, Refs. [24, 58] discuss extensions of the theory to include thermoelectric effects from electron-hole asymmetry, the implications of which in this framework are so far not studied in superconductors. Ref. [24] also derives other higher-order electron-hole symmetry breaking terms that are allowed and in principle present already for the parabolic electron dispersion, and may be important when the leading terms vanish. More generally, one can also study effective actions where all symmetry-allowed terms are included. [59] The approach here can be straightforwardly adapted to solving such actions numerically on the saddle-point level, without requiring much manual work.

The computer program used in this manuscript is available 45.

ACKNOWLEDGMENTS

I thank S. Ilić, F. S. Bergeret, and T. T. Heikkilä for discussions. This work was supported by European Union's HORIZON-RIA programme (Grant Agreement No. 101135240 JOGATE).

[1] E. Bauer and M. Sigrist, eds., *Non-centrosymmetric superconductors*, Lecture notes in physics, Vol. 847

(Springer, 2012).

[2] M. Smidman, M. Salamon, H. Yuan, and D. Agterberg, Superconductivity and spin-orbit coupling in non-centrosymmetric materials: a review, *Rep. Progr. Phys.* **80**, 036501 (2017).

[3] V. M. Edelstein, Magnetoelectric effect in polar superconductors, *Phys. Rev. Lett.* **75**, 2004 (1995).

[4] S. K. Yip, Two-dimensional superconductivity with strong spin-orbit interaction, *Phys. Rev. B* **65**, 144508 (2002).

[5] V. M. Edelstein, Magnetoelectric effect in dirty superconductors with broken mirror symmetry, *Phys. Rev. B* **72**, 172501 (2005).

[6] S. Yip, Noncentrosymmetric superconductors, *Annu. Rev. Condens. Matter Phys.* **5**, 15 (2014).

[7] F. Konschelle, I. V. Tokatly, and F. S. Bergeret, Theory of the spin-galvanic effect and the anomalous phase shift φ_0 in superconductors and Josephson junctions with intrinsic spin-orbit coupling, *Phys. Rev. B* **92**, 125443 (2015).

[8] A. Buzdin, Direct coupling between magnetism and superconducting current in the Josephson φ_0 junction, *Phys. Rev. Lett.* **101**, 107005 (2008).

[9] V. Barzykin and L. P. Gor'kov, Inhomogeneous stripe phase revisited for surface superconductivity, *Phys. Rev. Lett.* **89**, 227002 (2002).

[10] O. Dimitrova and M. V. Feigel'man, Theory of a two-dimensional superconductor with broken inversion symmetry, *Phys. Rev. B* **76**, 014522 (2007).

[11] D. Agterberg and R. Kaur, Magnetic-field-induced helical and stripe phases in Rashba superconductors, *Phys. Rev. B* **75**, 064511 (2007).

[12] F. Ando, Y. Miyasaka, T. Li, J. Ishizuka, T. Arakawa, Y. Shiota, T. Moriyama, Y. Yanase, and T. Ono, Observation of superconducting diode effect, *Nature* **584**, 373 (2020).

[13] C. Baumgartner, L. Fuchs, A. Costa, S. Reinhardt, S. Gronin, G. C. Gardner, T. Lindemann, M. J. Manfra, P. E. Faria Junior, D. Kochan, *et al.*, Supercurrent rectification and magnetochiral effects in symmetric Josephson junctions, *Nat. Nanotech.* **17**, 39 (2022).

[14] R. Wakatsuki and N. Nagaosa, Nonreciprocal current in noncentrosymmetric Rashba superconductors, *Phys. Rev. Lett.* **121**, 026601 (2018).

[15] A. Daido, Y. Ikeda, and Y. Yanase, Intrinsic superconducting diode effect, *Phys. Rev. Lett.* **128**, 037001 (2022).

[16] S. Ilić and F. S. Bergeret, Theory of the supercurrent diode effect in Rashba superconductors with arbitrary disorder, *Phys. Rev. Lett.* **128**, 177001 (2022).

[17] J. J. He, Y. Tanaka, and N. Nagaosa, A phenomenological theory of superconductor diodes, *New J. Phys.* **24**, 053014 (2022).

[18] M. Davydova, S. Prembabu, and L. Fu, Universal Josephson diode effect, *Science Adv.* **8**, eab0309 (2022).

[19] M. Nadeem, M. S. Fuhrer, and X. Wang, The superconducting diode effect, *Nature Rev. Phys.* **5**, 558 (2023).

[20] G. Eilenberger, Transformation of Gorkov's equation for type II superconductors into transport-like equations, *Z. Phys.* **214**, 195 (1968).

[21] K. D. Usadel, Generalized diffusion equation for superconducting alloys, *Phys. Rev. Lett.* **25**, 507 (1970).

[22] M. Houzet and J. S. Meyer, Quasiclassical theory of disordered Rashba superconductors, *Phys. Rev. B* **92**, 014509 (2015).

[23] I. V. Tokatly, Usadel equation in the presence of intrinsic spin-orbit coupling: A unified theory of magnetoelectric effects in normal and superconducting systems, *Phys. Rev. B* **96**, 060502 (2017).

[24] P. Virtanen, F. S. Bergeret, and I. V. Tokatly, Nonlinear σ model for disordered systems with intrinsic spin-orbit coupling, *Phys. Rev. B* **105**, 224517 (2022).

[25] T. H. Kokkeler, A. A. Golubov, and F. S. Bergeret, Field-free anomalous junction and superconducting diode effect in spin-split superconductor/topological insulator junctions, *Phys. Rev. B* **106**, 214504 (2022).

[26] S. Ilić, P. Virtanen, D. Crawford, T. T. Heikkilä, and F. S. Bergeret, Superconducting diode effect in diffusive superconductors and Josephson junctions with Rashba spin-orbit coupling (2024), arXiv:2406.17046.

[27] P. Virtanen, F. S. Bergeret, and I. V. Tokatly, Magnetoelectric effects in superconductors due to spin-orbit scattering: Nonlinear σ -model description, *Phys. Rev. B* **104**, 064515 (2021).

[28] F. Wegner, The mobility edge problem: Continuous symmetry and a conjecture, *Z. Phys. B* **35**, 207 (1979).

[29] K. Efetov, A. Larkin, and D. Khmel'nitskii, Interaction of diffusion modes in the theory of localization, *Zh. Eksp. Teor. Fiz.* **79**, 1120 (1980), [JETP **52**(3), 568 (1980)].

[30] A. M. Finkel'shtein, Superconducting transition temperature in amorphous films, *JETP Lett.* **45**, 46 (1987).

[31] D. Belitz and T. R. Kirkpatrick, The Anderson-Mott transition, *Rev. Mod. Phys.* **66**, 261 (1994).

[32] M. V. Feigel'man, A. I. Larkin, and M. A. Skvortsov, Keldysh action for disordered superconductors, *Phys. Rev. B* **61**, 12361 (2000).

[33] V. Mineev and G. Volovik, Electric dipole moment and spin supercurrent in superfluid ^3He , *J. Low Temp. Phys.* **89**, 823 (1992).

[34] H. Mathur and A. D. Stone, Quantum transport and the electronic Aharonov-Casher effect, *Phys. Rev. Lett.* **68**, 2964 (1992).

[35] J. Fröhlich and U. M. Studer, Gauge invariance and current algebra in nonrelativistic many-body theory, *Rev. Mod. Phys.* **65**, 733 (1993).

[36] P.-Q. Jin, Y.-Q. Li, and F.-C. Zhang, $\text{SU}(2) \times \text{U}(1)$ unified theory for charge, orbit and spin currents, *J. Phys. A: Math. Gen.* **39**, 7115 (2006).

[37] B. A. Bernevig, J. Orenstein, and S.-C. Zhang, Exact $\text{SU}(2)$ symmetry and persistent spin helix in a spin-orbit coupled system, *Phys. Rev. Lett.* **97**, 236601 (2006).

[38] I. V. Tokatly, Equilibrium spin currents: Non-abelian gauge invariance and color diamagnetism in condensed matter, *Phys. Rev. Lett.* **101**, 106601 (2008).

[39] C. Gorini, P. Schwab, R. Raimondi, and A. L. Shchepetkov, Non-Abelian gauge fields in the gradient expansion: Generalized Boltzmann and Eilenberger equations, *Phys. Rev. B* **82**, 195316 (2010).

[40] In some works, a convention where Nambu-offdiagonal elements of Q are Matsubara-antidiagonal is used. Mapping $Q \mapsto UQU$, $U(\omega, \omega') = \text{diag}(\delta_{\omega, \omega'}, \delta_{\omega, -\omega'})$ transforms between the conventions, with $\text{tr } \omega Q \mapsto \text{tr } \omega \tau_3 Q$.

[41] A. Altland, B. D. Simons, and D. T. Semchuk, Field theory of mesoscopic fluctuations in superconductor-normal-metal systems, *Adv. Phys.* **49**, 321 (2000).

[42] M. Y. Kupriyanov and V. F. Lukichev, Influence of boundary transparency on the critical current of dirty ss's structures, *Sov. Phys. JETP* **67**, 1163 (1988).

[43] P. Virtanen, A. Ronzani, and F. Giazotto, Spectral characteristics of a fully superconducting squipt, *Phys. Rev. Appl.* **6**, 054002 (2016).

- [44] K. K. Likharev, Superconducting weak links, *Rev. Mod. Phys.* **51**, 101 (1979).
- [45] P. Virtanen, (2024), ancillary files and <https://gitlab.jyu.fi/jyucmt/usadelndsoc>.
- [46] R. Gupta, Introduction to lattice QCD (1998), arXiv:hep-lat/9807028.
- [47] B. Bell, CppAD: a package for C++ algorithmic differentiation (2024), version 20240000.5.
- [48] H. Monien, Gaussian quadrature for sums: a rapidly convergent summation scheme, *Math. Comp.* **79**, 857 (2010).
- [49] D. A. Knoll and D. E. Keyes, Jacobian-free newton-krylov methods: a survey of approaches and applications, *J. Comp. Phys.* **193**, 357 (2003).
- [50] T. A. Davis, Algorithm 832: UMFPACK v4.3 — an unsymmetric-pattern multifrontal method, *ACM Trans. Math. Softw.* **30**, 196 (2004).
- [51] F. S. Bergeret and I. V. Tokatly, Theory of the magnetic response in finite two-dimensional superconductors, *Phys. Rev. B* **102**, 060506 (2020).
- [52] J. Pearl, Current distribution in superconducting films carrying quantized fluxoids, *Appl. Phys. Lett.* **5**, 65 (1964).
- [53] J. Sinova, S. O. Valenzuela, J. Wunderlich, C. H. Back, and T. Jungwirth, Spin Hall effects, *Rev. Mod. Phys.* **87**, 1213 (2015).
- [54] J.-i. Inoue, G. E. W. Bauer, and L. W. Molenkamp, Suppression of the persistent spin hall current by defect scattering, *Phys. Rev. B* **70**, 041303 (2004).
- [55] E. G. Mishchenko, A. V. Shytov, and B. I. Halperin, Spin current and polarization in impure two-dimensional electron systems with spin-orbit coupling, *Phys. Rev. Lett.* **93**, 226602 (2004).
- [56] A. Hijano, S. Vosoughi-nia, F. S. Bergeret, P. Virtanen, and T. T. Heikkilä, Dynamical hall responses of disordered superconductors, *Phys. Rev. B* **108**, 104506 (2023).
- [57] F. S. Bergeret, M. Silaev, P. Virtanen, and T. T. Heikkilä, Colloquium: Nonequilibrium effects in superconductors with a spin-splitting field, *Rev. Mod. Phys.* **90**, 041001 (2018).
- [58] G. Schwiete, Nonlinear sigma model with particle-hole asymmetry for the disordered two-dimensional electron gas, *Phys. Rev. B* **103**, 125422 (2021).
- [59] T. Kokkeler, F. S. Bergeret, and I. Tokatly, A universal phenomenology of charge-spin interconversion and dynamics in diffusive systems with spin-orbit coupling, arXiv:2405.06334 (2024).